

18 GHz REVERSE CHANNEL HEMT OSCILLATOR

Fatima Salete Correra & Edmar Camargo

Laboratório de Microeletrônica, Escola Politécnica - USP
 Cx. Postal - 8174 01051 - São Paulo - SP - Brazil

ABSTRACT

A simple analytical equation is proposed for describing the HEMT drain current and has been implemented at the SPICE simulator. It accurately modeled the HEMT transconductance compression and was applied to non-linear circuit simulation without convergence problems. Using this equation an oscillator design approach combining linear and non-linear analysis was used to design a DRO operating at 18 GHz employing a HEMT in the reverse channel configuration. The performance of the oscillator constructed confirmed the main results predicted by the simulations. The oscillator constructed generated +11 dBm at 18 GHz, and the circuit/device interaction predicted by the simulation was experimentally confirmed.

INTRODUCTION

The application of HEMT devices in large-signal circuits has recently been introduced [1,2] with promising results. This is a direct consequence of the HEMT device technology maturing and of the successful work on accurate non-linear device modelling. However, there is still a lack of experimental work on HEMT oscillator and of theoretical results employing non-linear simulators.

This paper presents a modified equation for the HEMT drain current to be used in the SPICE time domain simulator. This model is applied to study the performance of a reverse channel oscillator and its interaction with the external circuit. The simulation results are employed in the design of an 18 GHz DRO using a 0.5 μ m gate length HEMT on reverse channel configuration.

NON-LINEAR MODEL

At the present time, equivalent circuit models [3,4] for MESFETs implemented on SPICE are available to simulate the large-signal behaviour of a

broad range of non-linear circuits. Nevertheless, the application of these models to HEMTs is restricted, since this device presents differences when compared to MESFETs, mainly on its transfer characteristics [5].

In this paper a simple analytic equation, to be used on SPICE, is introduced for describing the HEMT drain current source, which is capable of representing the device transconductance with good accuracy. This equation results from a modification of the $I_d(V_{gs}, V_{ds})$ expression proposed by Statz et al [4] to model MESFETs drain current. It has been observed that the Statz equation can be used to model the HEMT for gate-source voltages within the threshold, V_T and the peak transconductance gate voltage, V_c . However for gate-source voltages greater than V_c , the drain current equation must be modified in order to properly represent the HEMT transconductance compression. This is accomplished by multiplying the former equation by a term employing an exponential function, resulting expression (1).

$$I_d(V_{gs}, V_{ds}) = \frac{1}{1 + A \cdot \exp(D \cdot V_{gs})} \cdot \frac{B \cdot (V_{gs} - V_T)^2}{1 + b \cdot (V_{gs} - V_T)} \cdot F(V_{ds}) \quad (1)$$

Where,

$$F(V_{ds}) = \left[1 - \left[1 - \frac{\alpha V_{ds}}{3} \right]^3 \right] \cdot [1 + \lambda V_{ds}] \quad \text{for } V_{ds} < 3/\alpha$$

$$F(V_{ds}) = [1 + \lambda V_{ds}] \quad \text{for } V_{ds} \geq 3/\alpha$$

The HEMT non-linear equivalent circuit used herein including package parasitics is presented in figure 1. It contains, besides the drain current nonlinearity three additional non-linear elements: the gate-source and gate-drain diodes and the gate-source capacitance. Although the diode current equation used for MESFETs is not

adequate for HEMTs, it has been employed since the effect of diode conduction may be neglected when simulating class A oscillators.

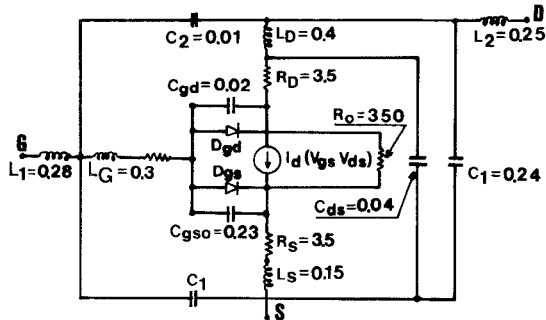


Fig. 1 - Common-source large-signal HEMT model (Capacitances are in pF, Resistances in Ohms, and inductances in nH).

The gate-source capacitance, C_{gs} was approximated by the capacitance of a reversed Schottky diode [5], described by equation (2).

$$C_{gs}(V_{gs}) = \frac{C_{gso}}{(1 + V_{gs}/V_{bi})^m} \quad (2)$$

The model of figure 1 was used to simulate the HEMT 2SK677 using SPICE. This device manufactured by SONY, presents a gate area of $0.5 \times 300 \mu\text{m}^2$ and an output power greater than 10 dBm at 12 GHz.

In order to extract the parameters of the HEMT model, DC and S-parameters were carried out [6] along with fitting techniques. The values of the model elements are on table I.

$A = 2.42$	$\lambda = 0.1$
$D = 0.95$	$V_T = -0.95 \text{ V}$
$b = 0.00$	$V_{bi} = 0.80 \text{ V}$
$\alpha = 5.20$	$C_{gso} = 0.23 \text{ pF}$
$\beta = 115E-3$	$m = 0.474$

Table I - Elements of the non-linear model.

The ability of the model to predict the actual common source drain current in function of gate voltage is shown in figure 2(a), which compares the measured and theoretical results. The comparison is more evident when derivatives are made, which is the case of the transconductance represented in figure 2(b). The

transconductance calculated from the Statz model is depicted in the same figure.

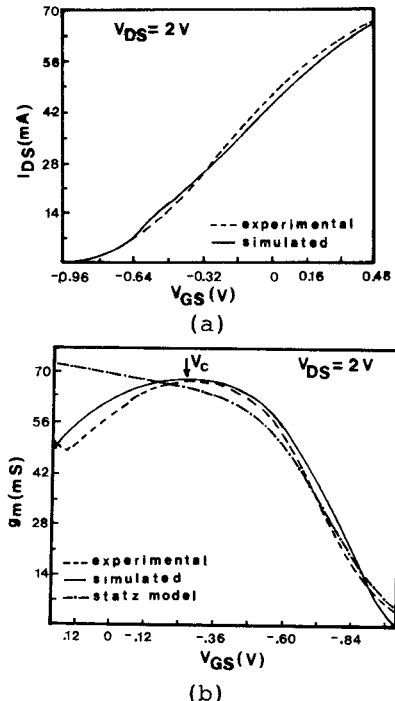


Fig. 2 - Main static characteristics:
(a) Drain current x gate-source voltage,
(b) Transconductance.

Based on experimental data [6] the output resistance was set to its high frequency value at the saturated region by means of a fixed resistance R_o .

To model the HEMT at reverse channel configuration the package parasitics was kept as in the common source model, but the intrinsic transistor had its source and drain connections interchanged as in the common drain case. This approach implicitly assumes that the transistor is symmetrical.

OSCILLATOR DESIGN AND SIMULATION

The approach used to design the oscillator consists of a small-signal analysis to determine the basic oscillator circuit, followed by a large-signal analysis to optimize the load for maximum output power. This approach was employed in the design of a dielectric resonator oscillator at 18 GHz.

The linear analysis started by calculating the S-parameters for the HEMT in the reverse channel configuration biased for maximum transconductance. Under these conditions it was found that the device was potentially unstable from 10 to 20 GHz. An open stub resonator was then added to the gate and had its length set to maximize the

reflection coefficient amplitude, $|S_{22}|$ at the drain terminal. Applying this procedure the drain terminal presented a linear impedance equal to $-29 - j40$ ohms.

The non-linear analysis was then applied to the circuit in order to find out the resistive load that gives the maximum power output. The oscillation condition at the drain port was imposed from the linear analysis results, resonating the reactive part of its impedance at the operating frequency for several values of resistive loads. The simulated results are presented in figure 3, and the maximum output power occurs for a load resistance of 15 ohms, half the value of the negative resistance predicted by linear analysis.

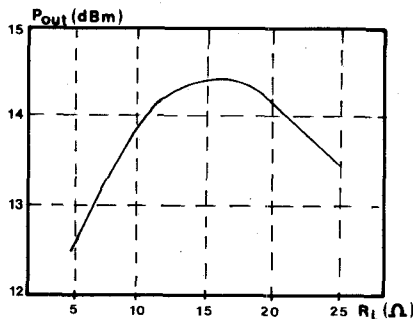


Fig. 3 - Output power x load resistance.

The dynamic drain current \times voltage trajectory at the intrinsic HEMT was simulated for the maximum power condition. The results are represented in figure 4 on the theoretical static $I_D \times V_D$ characteristics. It is depicted in this figure the slight invasion of the RF signal on the region of gate conduction for a very short period of time in the order of 10% of a RF cycle. This confirms the assumption that the effect of diode conduction may be neglected.

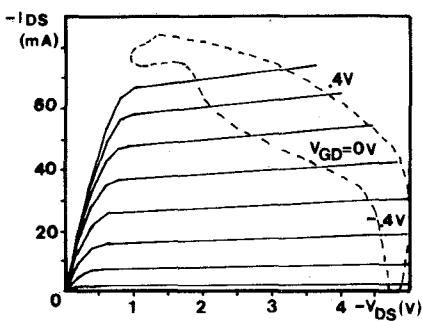


Fig. 4 - Dynamic current x voltage trajectory.

OSCILLATOR CONSTRUCTION AND RESULTS

The experimental verification of the predicted results started with the investigation of the oscillating bandwidth

potential. Stable oscillations were obtained from 10 to 22 GHz, by changing the dielectric resonator at the gate circuit and empirically tuning the output. This result confirms that the circuit has the potential of being relatively broadband.

The HEMT oscillator was implemented in microstrip on 0.25 mm thick soft substrate with $\epsilon_r = 2.2$. The structure of the experimental oscillator is depicted in figure 5. It is shown that the gate open stub resonator was replaced by a dielectric resonator which is more practical to use when advantages such as high Q, tuning flexibility and elimination of instabilities at low frequencies are considered.

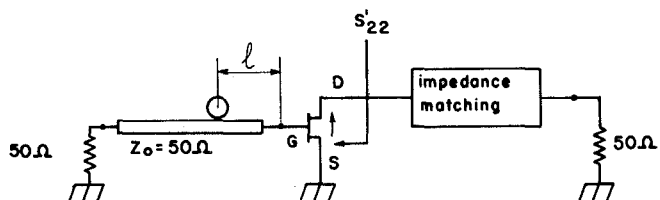


Fig. 5 - Reverse channel oscillator structure.

The matching circuit consists of a series line cascaded with a double open stub. This simple circuit is capable of resonating the reactive part of the drain impedance as well as to provide the required resistive load. The photograph of the oscillator is presented in figure 6.

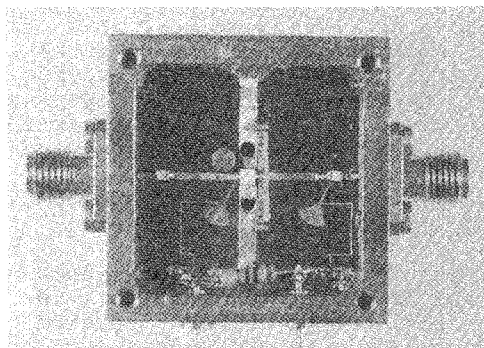


Fig. 6 - Photo of the oscillator.

In the next step, the resonator was fixed within the circuit, at the position predicted for oscillating at 18 GHz. The matching circuit designed for presenting the oscillating conditions, was connected to the drain and the circuit promptly started oscillating at 17.9 GHz. The screw located in the upper lid was used for tuning the dielectric resonator to bring the frequency to the expected value. The

output power at this frequency was in the order of + 11 dBm. The difference between predicted and measured output power may partially be attributed to losses at the dielectric resonator and power leakage to the gate load (1 dB) and losses in the output circuit (1 dB). The remaining power difference is due to the inability of the model to account for all the non-linear effects and circuit unaccuracies.

Final important experimental results are the DC to RF efficiency, in the order of 10 % and the phase noise characteristic presented in figure 7.

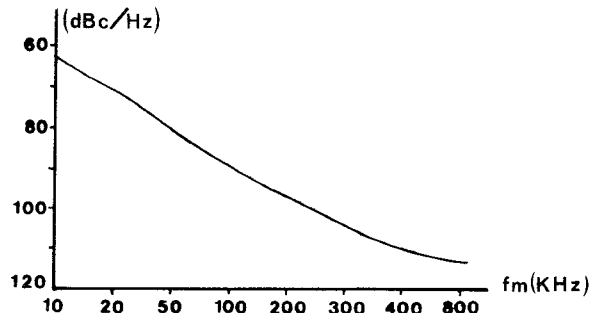


Fig. 7 - Oscillator phase noise.

CONCLUSIONS

The equation proposed for the drain current of the HEMT presented good accuracy to fit its static I_xV and transconductance characteristics. It was successfully implemented in SPICE program, enabling non-linear circuit simulation to be carried out without convergence problems. The application of the HEMT modeling to the design of a reverse channel HEMT oscillator was useful to determine the optimum oscillating conditions for maximum output power. Experimental results obtained from the oscillator constructed confirmed many of the simulated predictions, encouraging the continuity of the HEMT model development to include additional non-linear effects.

The electrical performance obtained for the 18 GHz oscillator was + 11 dBm with 10% efficiency. The reverse channel configuration looks attractive for HEMT oscillators, due to its potential of generating microwave power in a wide frequency band.

ACKNOWLEDGEMENTS

The authors wish to acknowledge the contribution of F. Colombani on transistor modeling. Acknowledgements are also due to TELEBRAS R & D Center for supplying the active devices. This work received the financial support of the following

brazilian entities: FINEP - Financiadora de Estudos e Projetos, FAPESP - Fundação de Amparo a Pesquisa do Est. São Paulo, CNPq - Conselho Nacional de Desenvolvimento Científico e Tecnológico and CAPES - Coord. de Aperfeiçoamento de Pessoal de Nível Superior.

REFERENCES

- [1] M. Sholley, S. Mass, B. Allen, R. Sawires, A. Nichols and J. Abell, "HEMT mm-Wave Amplifiers, Mixers and Oscillators", *Microwave Journal*, pp 121-131, 1985.
- [2] P. Bura and B. Vassilakis, "A Balanced 11 GHz HEMT Up-converter", *1989 IEEE MTT-S Int. Micr. Symp. Digest*, Vol III, pp 1299-1302, 1989.
- [3] W. R. Curtice and M. Ettenberg, "A Nonlinear GaAs FET Model for Use in the Design of Output Circuits for Power Amplifiers", *IEEE Trans. on Micr. Theo. and Techniques*, Vol MTT-33, No 12, pp 1383-1393, 1985.
- [4] H. Statz, P. Newman, I. W. Smith, R. A. Pucel and H. A. Haus, "GaAs FET Device and Circuit Simulation in SPICE", *IEEE Trans. on Elec. Devices*, Vol ED-34, No 2, pp 160-169, 1987.
- [5] G. Wang, I. Ichitsubo, W. H. Ku, Y. Chen and L. F. Eastman, "Large-Signal Time-Domain Simulation of HEMT Mixers", *IEEE Trans. on Theo. and Techniques*, vol 36 No 4, pp 756-758, 1988.
- [6] D. Consoni, M. Cordaro and E. Camargo, "Dependence of HEMT Microwave Performance on Bias Regions", *Symp. Proc. - 1989 SBMO Int. Micr. Symp.*, pp 785-790.